ACS ENGINEERING Au
AN OPEN ACCESS JOURNAL OF THE AMERICAN CHEMICAL SOCIETY

pubs.acs.org/engineeringau
Article

Effect of pH Value on the Electrical Properties of PEDOT:PSS-Based Fiber Mats

Published as part of the ACS Engineering Au virtual special issue "Materials Design".

Prerana Rathore and Jessica D. Schiffman*

Cite This: *ACS Eng. Au* 2023, 3, 527−536
Read Online

ABSTRACT: Nanofiber mats containing poly(3,4-ethylenedioxythiophene) (PEDOT) hold potential for use in wearable electronic applications. Unfortunately, the use of PEDOT is often limited by the acidic nature of polystyrenesulfonate (PSS), a common dispersant for PEDOT. In this study, we explored the impact of increasing the pH value of PEDOT:PSS/poly(vinyl alcohol) (PVA) precursors on the morphological and electrical properties of the resultant electrospun fibers. Specifically, electrospun nanofibers were analyzed using scanning electron microscopy, bright-field microscopy, and two-point probe measurements. We discovered that neutral and even slightly basic PEDOT:PSS/PVA precursors could be electrospun without affecting the resultant electrical properties. While cross-linking effectively stabilized the fibers, their electrical properties decreased after exposure to solutions with pH values between 5 and 11, as well as with agitated soap washing tests. Additionally, we report that the fiber mats maintained their stability after more than 3000 cycles of voltage application. These findings suggest that PEDOT:PSS-based fibers hold potential for use in wearable textile and sensor applications, where long-term durability is needed.

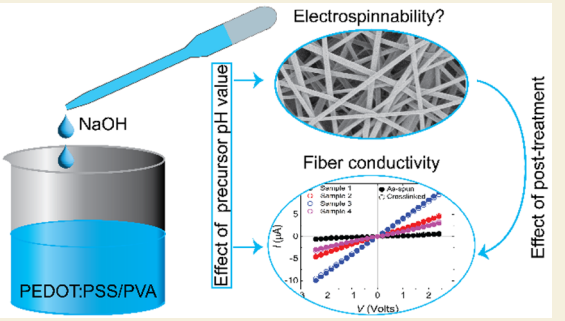

KEYWORDS: *Electrospinning, Electrical conductivity, PEDOT:PSS, pH, Textiles, Wearables*

INTRODUCTION

Electrically conductive fiber mats are ideal for applications, such as sensors,[1−4] artificial skin,[5−7] and wearable textiles[8] due to their surface-to-volume ratio, porosity, stretchability, and mechanical strength.[9] Electrospinning is the most common method of fabricating fiber mats due to its ease of use, control over fiber diameter and morphology, production of continuous fibers, facile functionalization of fibers, and scalability.[10−12] To obtain conductive fibers via electrospinning, typically conductive additives, such as carbon nanotubes,[13,14] metal nanowires,[15] and/or conjugated polymers,[16,17] are blended with a carrier polymer to facilitate fiber formation. If the conductive additive is not as flexible as the polymer matrix, then the composites can fail due to mechanical mismatch (i.e., interfacial slipping, cracking, etc.)[14] To avoid mismatch, an alternative method is to use a flexible conjugated polymer within the composite, such as polyalanine, polypyrrole, or poly(3,4-ethylenedioxythiophene) (PEDOT).

PEDOT has been widely explored due to its high and stable electrical conductivity, ease of doping, good photo- and electrical stability in air, as well as high work function and transmittance.[18,19] Notably, the synthesis procedure of PEDOT affects its conductivity and dispersibility.[20] While the most common method for synthesizing PEDOT is oxidative chemical polymerization, other methods, such as electrochemical polymerization and transition metal-mediated coupling polymerization have also been used.[18,21] Unfortunately, working with PEDOT can be challenging because it has limited dispersibility in solvents. Therefore, in most common commercial syntheses, EDOT is polymerized in the presence of a water-soluble polyanion, i.e., polystyrenesulfonate (PSS). PSS disperses and stabilizes PEDOT by forming colloidal particles containing a higher number of PSS chains at the periphery and a higher number of PEDOT chains at the core.[22] Due to its electrical properties, PEDOT:PSS-based electrospun fibers have been used in various applications, including gas sensors that detect organic vapors,[23] carbon monoxide,[24] ammonia,[25] and hydrogen gas,[26] as well as strain[27,28] and humidity sensors;[29] and thermoelectric devices.[30−32] In most of these studies, PEDOT:PSS was blended with a non-conducting carrier polymer, such as poly(vinyl alcohol)

Received: August 21, 2023
Revised: October 6, 2023
Accepted: October 10, 2023
Published: October 31, 2023

(PVA),[33−35] polyvinylpyrrolidone (PVP),[30] or poly(ethylene oxide) (PEO)[33,36] to improve the electrospinnability. In one study by Huang et al.,[23] the carrier polymer was avoided by blending PEDOT:PSS with a small amount of magnesium nitrate that acted as a thickener to facilitate electrospinning. There are other studies that used coaxial electrospinning; in these, the optical and electrical properties of fibers containing PEDOT:PSS in the core[37,38] or in the shell[38] were evaluated.

The electrical performance of single nozzle electrospun PEDOT:PSS-based fiber mats has been explored in many studies. For example, Park et al.[33] electrospun PEDOT:PSS-based fibers and evaluated the effect of the carrier polymers (PEO or PVA) and cosolvents (dimethyl sulfoxide or ethylene glycol) on the electrical conductivity. PEDOT:PSS/PEO fibers had a higher conductivity than the PEDOT:PSS/PVA fibers because when PEO was used, the more conductive quinoid structure was in abundance, as indicated by a broad peak at 1430 cm^{-1} in the Raman spectra. Additionally, while ethylene glycol increased the conductivity more than dimethyl sulfoxide, using either solvent improved the conductivity of the PEDOT:PSS/PVA and PEDOT:PSS/PEO fibers, which was also supported by a broader peak in the Raman spectra. The conductivity of the as-spun PEDOT:PSS/PEO fibers was also improved after they were immersed in ethanol[39] or ethylene glycol[39,40] due to the removal of PEO and change in PEDOT conformation. In these studies, the use of PSS was essential in dispersing PEDOT in the appropriate solvents.

Due to the presence of sulfonic groups in PSS, commercial formulations of PEDOT:PSS dispersions have a pH value between 1.5 and 2.5.[41] This high acidity leads to corrosivity; for example, when PEDOT:PSS was deposited and dried as a hole-injecting layer on indium doped tin oxide (ITO) anode for light-emitting diodes, the ITO etched into the PEDOT:PSS layer due to the acidic nature of the latter.[42] The etching process has been observed in other systems as well and decreases the lifetime and performance of the devices significantly.[43,44] Therefore, in many studies, EDOT monomers are polymerized on the substrate producing a thin film of PEDOT without involving acidic PSS.[45] Another method to eliminate the adverse effects of PEDOT:PSS's acidity is to increase its pH value by mixing it with a base, such as sodium hydroxide (NaOH). For example, Mochizuki et al.[46] increased the pH value of PEDOT:PSS dispersions up to 13 by adding NaOH and found that the electrical conductivity of the cast thin films decreased as the pH value increased due to dedoping of PEDOT. While many strategies to overcome the adverse effects caused by the acidity of PSS have been reported for thin films,[47] only one strategy has been explored for electrospun fibers.[48−50] This involved the polymerization of EDOT monomers within or onto fibers to enhance their biocompatibility as well as their electrical and mechanical properties. Moreover, for the more common PEDOT:PSS-based fibers, there are no studies that discuss how altering the pH value of these commercial precursors impacts the final morphological or electrical properties of the electrospun fibers. Furthermore, many applications, such as *in vivo* sensors, require the conductive fibers to be used in different pH environments and to-date no studies have investigated how exposing PEDOT:PSS-based fibers to different environments impacts their properties.

In the current work, we examined the effect of increasing the pH value of PEDOT:PSS-based precursors from ∼2.5 to ∼12 on the electrospinnability and electrical properties of the resulting fiber mats. For PEDOT:PSS-based fibers to be appropriate for applications, it is important to understand their long-term performance and stability in various environments in which they might be used. For this reason, we also cross-linked the mats and evaluated if their electrical conductivity changed after submersion in solutions with various pH values, as well as after multiple rounds of washing tests featuring soapy water. The electrical conductivity of as-spun fiber mats over multiple months and 3000 current−voltage scans was also evaluated. This study demonstrates that the electrical properties of PEDOT:PSS-based fibers persist when electrospun from a wide range of pH values and after application of multiple current−voltage cycles, making them suitable for a variety of applications, including wearable textiles and sensors.

MATERIALS AND METHODS

Materials and Chemicals

All chemicals were used as received. Poly(3,4-ethylenedioxythiophene):polystyrenesulfonate (PEDOT:PSS) was purchased from Sigma-Aldrich as a dispersion in water with 1.3 wt % solid content (0.5 wt % PEDOT and 0.8 wt % PSS) and a reported conductivity of 1 S/cm. Acetic acid, glutaraldehyde solution (50 wt % in water), and Mowial 18-88 poly(vinyl alcohol) (PVA) with a molecular weight of 130 kDa and degree of hydrolysis of 87−89% were also purchased from Sigma-Aldrich. Sodium hydroxide (NaOH), acetone, Sparkleen 1, sodium iodide (NaI), sodium bromide (NaBr), sodium chloride (NaCl), and magnesium chloride ($MgCl_2$) were purchased from Fisher Scientific. Deionized (DI) water was obtained from a Barnstead Nanopure Infinity water purification system (Thermo Fisher Scientific, Waltham, MA).

Fisherbrand microscope glass slides were purchased from Fisher Scientific. Interdigitated electrodes (IDEs) consisted of 20 platinum electrodes (10 pairs) that were 50 nm thick and 4.5 mm in length, with a 100 μm spacing (Figure S1A). The IDEs were fabricated in Dr. Jun Yao's Laboratory (Department of Electrical and Computer Engineering, UMass Amherst) on Si wafers (N-Type, P doped, single-side polished with 1 μm thermal oxide layer purchased from University Wafer, Boston, MA). Then, a 30-gauge (0.31 mm) copper wire was attached to each electrode by using silver conductive epoxy adhesive (MG Chemicals).

Preparation of PEDOT:PSS/PVA Precursors

An aqueous PVA solution (20 wt %) was obtained by mixing PVA with water at 60 °C for 48 h on a magnetic hot plate (Corning Inc., Corning, NY). Next, the PVA solution was mixed with the PEDOT:PSS dispersion overnight at room temperature in 1:1.5 and 1:3 weight ratios using an end-overend mixer (Benchmark Scientific, Sayreville, NJ) at 20 rpm. The final concentrations of the PVA, PEDOT, and PSS in the precursors used in this study were (1) 8, 0.3, and 0.48 wt % and (2) 5, 0.375, and 0.6 wt %, which we will refer to as LowPEDOT and HighPEDOT, respectively. The pH values of the as-prepared LowPEDOT and HighPEDOT precursors were 2.6 and 2.4, respectively, as measured at room temperature using a Fisherbrand accumet AB 150 pH benchtop meter (Hampton, NH). NaOH pellets were added to the LowPEDOT and HighPEDOT precursors to explore the impact of changing the precursor pH value (from 5.3 to 12.0) on electrospinnability (see Table 1).

Electrospinning of PEDOT:PSS/PVA Fiber Mats

A precursor was loaded into a 5 mL Luer-Lock syringe (Norm-Ject, Tuttlingen, Germany) and capped with an 18-gauge hypodermic beveled-tip needle (Exelint, Redondo Beach, CA). The syringe was mounted to a horizontal syringe pump (Cole Parmer, Vernon Hills, IL) that delivered the precursor at a constant volumetric flow rate of 0.5 mL/h (Figure 1A). A copper plate, wrapped with aluminum (Al) foil and placed 15 cm away from the tip of the needle, was used as a collector. IDEs were attached to Al foil after subsequently rinsing with DI water and acetone followed by exposure to UV/Ozone (Bioforce

https://doi.org/10.1021/acsengineeringau.3c00044
ACS Eng. Au 2023, 3, 527−536

Table 1. Electrospun Fiber Mat Names and Electrospinning Precursor Compositions Used in this Study

fiber mat name	PEDOT:PSS/PVA (wt %:wt %/wt %)	PEDOT in final fibers (wt %)	precursor pH value
LowPEDOT3[a]			2.6
LowPEDOT5			5.3
LowPEDOT7	0.30:0.48/8	3.42	7.3
LowPEDOT8			8.5
LowPEDOT11			11.4
HighPEDOT2			2.4
HighPEDOT5			5.3
HighPEDOT7	0.38:0.60/5	6.28	7.3
HighPEDOT8			8.5
HighPEDOT12			12.0

[a]LowPEDOT3 was also cross-linked using glutaraldehyde vapor for 38 h and used in stability studies including exposure to solutions of various pH values and soapy water.

Nanosciences, Virginia Beach, VA) for 15−20 min. For electrospinning, the collector and the needle were connected to a high-voltage supply (Gamma High Voltage Research, Ormond Beach, FL), that was used to apply a high voltage of 25 kV. The entire electrospinning setup was placed inside an acrylic box with a controlled relative humidity of 21−23% that was maintained by passing air through Drierite desiccants. The electrospinning was carried out at room temperature (23−24 °C) for ∼30 min.

Stability Testing on Fiber Mats

As-spun LowPEDOT3 fiber mats collected on IDEs were cross-linked by exposure to glutaraldehyde vapor for 38 h[51,52] (see Figure 1B). These samples will be referred to as cross-linked fiber mats throughout the Results and Discussion. To evaluate the effect of exposing the cross-linked fiber mats to different pH environments, the mats were immersed in a NaOH/water (pH = 7, 11, or 14) or acetic acid/water (pH = 5) solution for 16 h followed by drying at 60 °C for 1 h (See Figure 1B). As one application of PEDOT:PSS-based fiber mats is wearable textiles, we examined if washing the cross-linked fiber mats with soapy water would affect their performance. The cross-linked fiber mats were washed by immersion in 1 wt % Sparkleen 1 (soapy water) and simultaneous mixing at 80 rpm using an orbital shaker (Fisher Scientific) for 1 h at room temperature. Then fiber mats were rinsed using DI water three times followed by heating at 60 °C for 1 h to dry them. For each fiber mat, at least two rounds of washing and drying were performed, and their electrical performance was re-evaluated after each round.

Visualization of PEDOT:PSS/PVA Fiber Mats

Scanning electron microscopy (SEM; FEI Magellan 400 XHR-SEM, Thermo Fisher Scientific, Waltham, WA) was used to determine the morphology and diameter of the as-spun fibers. Fibers were electrospun onto Al foil before being mounted on SEM stubs that were sputter coated (Cressington 208 Sputter Coater, Watford, UK) with 3 nm of platinum before imaging. The average fiber diameter and diameter distribution were calculated by measuring at least 50 random fibers within SEM micrographs using ImageJ software (version 1.53a). Microsoft Excel was used to conduct two-tailed, unpaired student's *t* tests to determine statistical significance, as will be mentioned in the Results and Discussion. Brightfield microscopy of IDEs was performed using Zeiss SteREO Discovery.V12 to determine the coverage and thickness of as-spun fiber mats. Moreover, to visualize the effect of cross-linking and immersion in aqueous solutions of various pH values, the cross-linked and immersed fiber mats were also imaged (see Figure 1B). Raman spectroscopy was performed using Horiba iHR320 Raman microscope equipped with a laser of 532 nm wavelength on fibers mats that were electrospun for 30 min on glass slides.

Electrical Measurements of PEDOT:PSS/PVA Fiber Mats

For electrical measurements under vacuum, the IDEs were placed inside an in-house-built environmental chamber that created a vacuum; the copper wires extended out of the chamber and were connected to a two-point probe (Signatone HS100 and Keithley S4200-SCS) (see Figure S1B). The electrical current was measured as a function of time for 20 s at each voltage from −2.5 to 2.5 V with a 0.1 V step. Then the average and the standard deviation in the electrical current were calculated over the last 15 s and reported as a function of voltage. Electrical measurements on the as-spun LowPEDOT3 fiber mats were also acquired as a function of relative humidity, from 30 to 90%. A Petri dish containing saturated aqueous

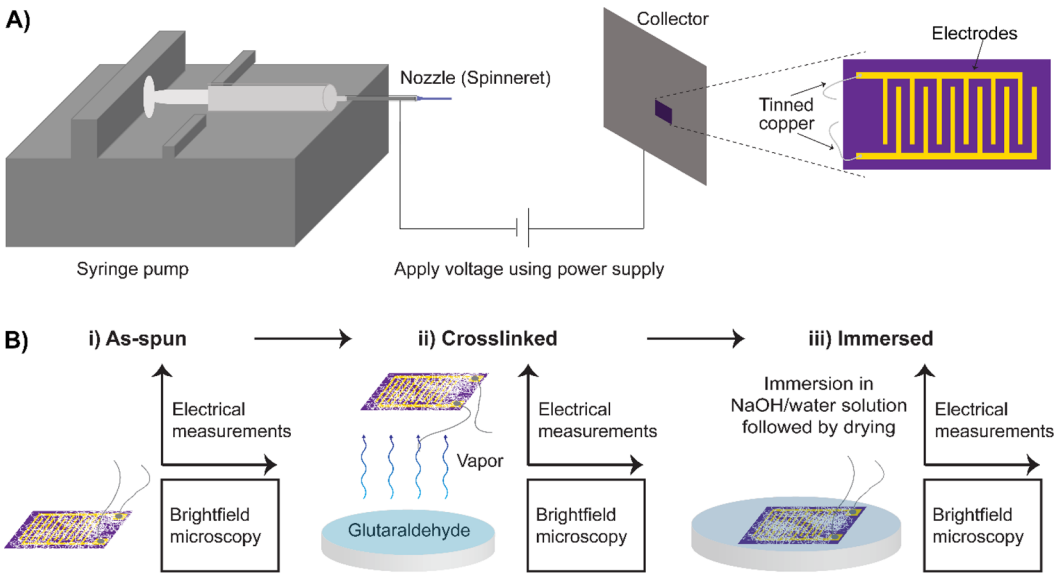

Figure 1. (A) In this study, conductive fibers were electrospun directly onto different substrates, including interdigitated electrodes (IDEs). (B) Schematic diagram showing the flow of experiments conducted in this study. (i) Fiber mats were electrospun on IDEs and their electrical and morphological properties were characterized using two-point probe measurements and brightfield microscopy, respectively. (ii) Fiber mats were cross-linked using glutaraldehyde vapor and recharacterized. (iii) The cross-linked fiber mats were immersed in either aqueous solutions with a pH value between 5 and 14 or soapy water, dried, and recharacterized.

https://doi.org/10.1021/acsengineeringau.3c00044
ACS Eng. Au 2023, 3, 527−536

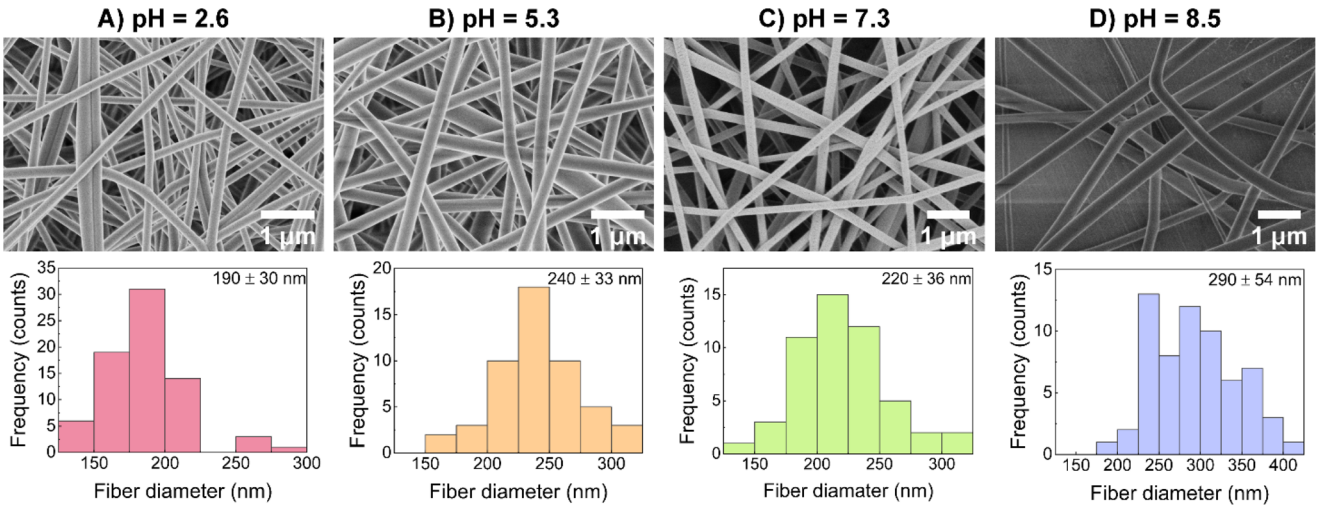

Figure 2. SEM micrographs and fiber diameter distribution for (A) LowPEDOT3, (B) LowPEDOT5, (C) LowPEDOT7, and (D) LowPEDOT8 fiber mats. The average diameter is shown in upper-right corner of the distribution graphs and the pH value of each precursor is also provided.

salt solutions was employed for various relative humidities, i.e., $MgCl_2$ for 33%, NaI for 38%, NaBr for 58%, NaCl for 75%, and pure water for >90%,[53] which was kept inside the environmental chamber overnight prior to acquiring electrical measurements, as previously described. To evaluate the electric performance over multiple current−voltage scans, a voltage sweep was used, and the current was measured at each voltage for 2 s under vacuum.

RESULTS AND DISCUSSION

Effect of Precursor pH on the Electrospinability and Morphology of PEDOT:PSS-Based Fiber Mats

We have successfully obtained electrospun fibers from PEDOT:PSS-based precursors as a function of different pH values, as outlined in Table 1. Uniform and smooth fibers with spherical cross sections (see Figure 2 and Table S1) that were electrospun from LowPEDOT3, LowPEDOT5, LowPEDOT7, and LowPEDOT8 precursors had average diameters of 190 ± 30, 240 ± 33, 220 ± 36, and 290 ± 54 nm, respectively. According to a paired two tailed t test, the fiber diameters were statistically different with $p < 10^{-3}$. It was observed that as the precursor's pH value increased, so did the solution viscosity, especially for the precursor that had a pH value of 8.5 (which also deposited fewer fibers). The increase in viscosity of PVA solutions with increasing pH value has been reported by Kasselkus et al.[54] When the viscosity of a precursor solution increases, it leads to increases in fiber diameter because the resistance to stretching increases.[55,56] When the pH value of the LowPEDOT precursor was further increased to 11.4, the precursor was gel-like (Figure S2) and could not be processed via electrospinning.

In contrast, the HighPEDOT precursors resulted in fibers with beads-on-a-string morphology across all pH values tested (Figure S3 and Table S1). When electrospun from a precursor with a pH value of 2.4, the average bead and fiber diameter were 400 ± 200 and 70 ± 13 nm, respectively (see Figure S4). The HighPEDOT precursors result in beads-on-string morphology was likely due to the lower concentration of the carrier polymer PVA. Typically, uniform fibers are obtained only when the concentration of the polymer is above entanglement concentration.[12,57] For HighPEDOT, as observed for LowPEDOT precursors, the fiber collection rate visually decreased at a pH value of 8.5; at a pH value of 12, the precursor was not electrospinnable due to gelation/precipitation (Figure S5).

Effect of Fiber Mat Thickness on Their Electrical Properties

The effect of fiber mat thickness on their electrical properties was explored by electrospinning LowPEDOT3 fiber mats with different thicknesses directly onto IDEs. We categorically named the fiber mats as thin, medium, thick, and very thick based on their transparency (see Figure 3). To evaluate their

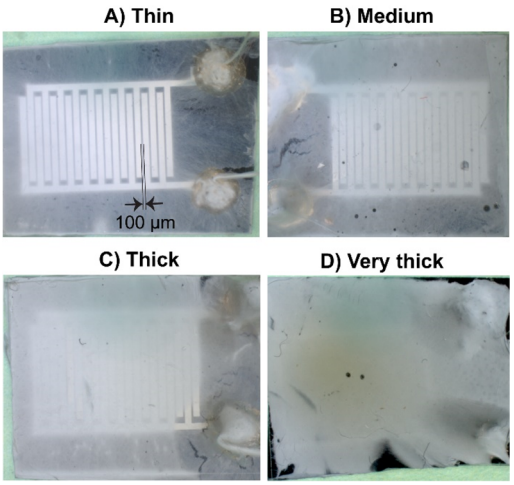

Figure 3. Brightfield microscopy images of as-spun fiber mats on IDEs were categorized as (A) thin, (B) medium, (C) thick, and (D) very thick based on their transparency. All fibers were electrospun from precursor LowPEDOT3. For scale, we note that the spacing between the electrodes is 100 μm.

electrical properties under vacuum, the current was measured as a function of time (see Figure S6) at each voltage between −2.5 to 2.5 V. As shown in Figure S6, the variation in the current (~0.002 μA) with time was much smaller than the average current (~3.66 μA), which implies that the current was constant with time at each voltage. Next, the average current was plotted as a function of voltage, as shown in Figure 4.

Figure 4 shows that no correlation between the electrical current and the thickness of the fiber mats was observed. For example, the electric current through the *Very thick 2* sample

https://doi.org/10.1021/acsengineeringau.3c00044
ACS Eng. Au 2023, 3, 527−536

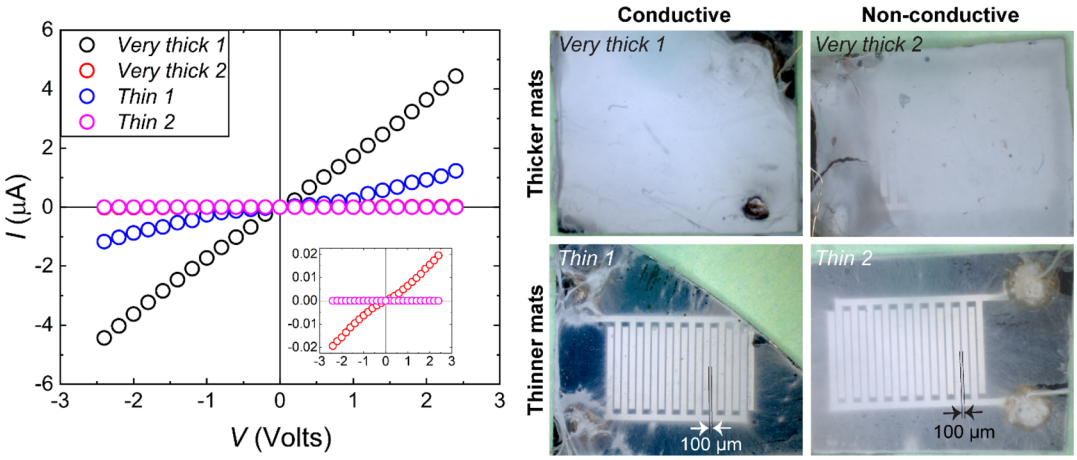

Figure 4. Current (I)−voltage (V) data and bright-field microscopy images of the LowPEDOT3 fiber mats tested. The inset shows current−voltage data for *Very thick 2* and *Thin 2* samples, as the current was too low to be visible in the main plot. For scale, we note that the spacing between the electrodes is 100 μm.

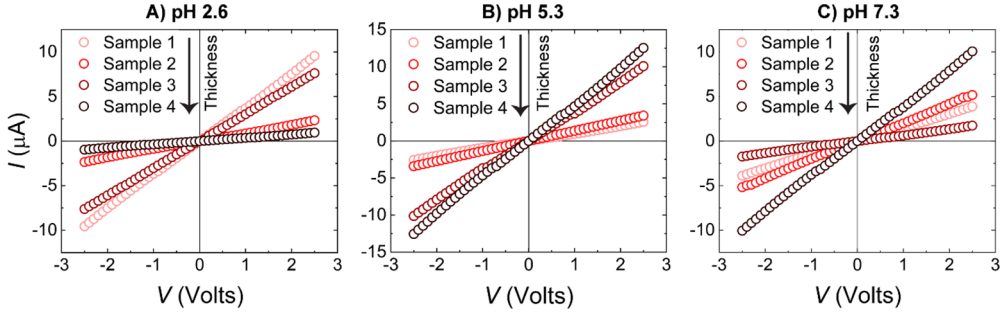

Figure 5. Current (I)−voltage (V) data measured under a vacuum for as-spun (A) LowPEDOT3, (B) LowPEDOT5, and (C) LowPEDOT7 fiber mats. The y and x axes represent electrical current (I) and voltage (V), respectively. In each case, the current was measured for 4 distinct fiber mats with different thicknesses. The thickness increased from sample 1 to sample 4. See Figures S7−S9 for the microscopy images of the fiber mats.

(0.02 μA at 2.4 V) was orders of magnitude smaller than those through the *Very thick 1* (4.4 μA at 2.4 V) and *Thin 1* (1.2 μA at 2.4 V). For sample *Thin 2*, the current was too low to be measured by using our two-point probe setup. We suggest that the reason for the disconnect between thickness and the electric current is due to the variation in adhesion of the fibers to IDEs, as well as interfiber packing within the mats. Poor adhesion leads to high contact resistance between mats and IDEs.

The adhesion of electrospun fibers on the collector depends on many factors, such as applied voltage during electrospinning, the thickness of the fiber mats, the conductivity and roughness of the collector, cross-linking process, thermal treatment, and surface interactions between the collector and fiber mats.[58−60] We observed that many of the thick fiber mats delaminated from the IDEs, possibly due to residual electric charge between fiber layers.[59,61] For such fiber mats, both the interlayer resistance and contact resistance increase with thickness. Hence, for fiber mats, unlike the films/sheet, the relationship between electrical current and thickness is not linear due to inconsistency in adhesion. Therefore, the calculations of true electrical conductivity require values for thickness and adhesion both of which are challenging to acquire; many thickness measurement techniques, such as ellipsometry and profilometry, cannot be used on rough and porous surfaces like fiber mats and incorporating the fiber adhesion values into the calculation for contact resistance is beyond the scope of this study. We note that using a 4-point probe setup would eliminate the need for contact resistance measurements; however, we did not have access to 4-point probe setup and the roughness of the fiber mats would remain a concern and lead to inaccurate electrical measurements. Nonetheless, the resistance of our well-adhered as-spun fiber mats (~0.1−2 MΩ) was similar to what other studies have obtained for similar PEDOT:PSS fiber mats.[35,39]

Electrical Properties of PEDOT:PSS-Based Fiber Mats Electrospun from Different pH Value Precursors

With the insight that producing well-adhered fiber mats is more important than obtaining electrospun mats with precisely the same thickness, we next selected well-adhered fiber mats to evaluate the effect that the precursor pH value had on the electrical current. Figures 5 and S7−S9 display the results for the LowPEDOT3, LowPEDOT5, and LowPEDOT7 fiber mats. We note that the current−voltage data are not shown for LowPEDOT8 fibers because, at this pH value, not enough fibers could be obtained on the IDEs for current measurements. The current at 2.5 V varied from 1 to 15 μA irrespective of the pH value of the precursor, indicating that the pH value of the precursor did not impact the electric current. This finding is consistent with prior studies involving films cast from pure PEDOT:PSS, which found that even though the conductivity decreased as the pH increased between pH 4 and 11, the decrement was not as significant as between pH values of 1 and 4 or above a pH value of 11.[46] However, directly comparing the conductivity of these fiber mats was not

https://doi.org/10.1021/acsengineeringau.3c00044
ACS Eng. Au 2023, 3, 527−536

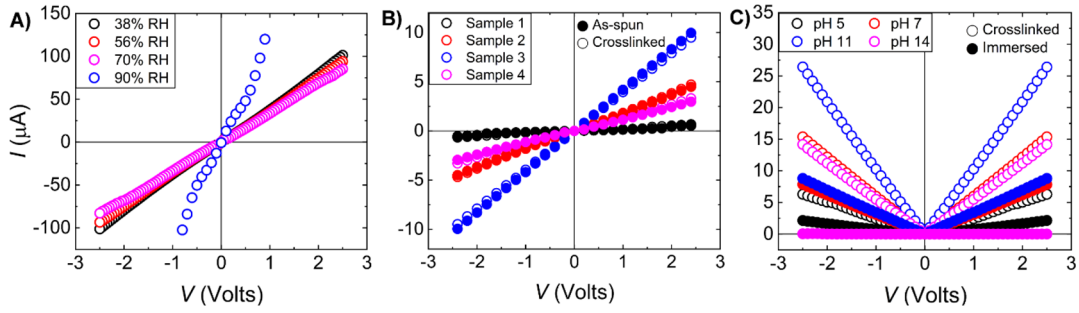

Figure 6. Current (I)−voltage (V) data for LowPEDOT3 fiber mats measured under vacuum. (A) Effect of relative humidity (RH) on as-spun fiber mats. (B) Effect of cross-linking on the conductivity of four different fiber mats. Filled and open circles represent as-spun and cross-linked fiber mats, respectively. (C) Conductivity of cross-linked fiber mats before and after immersion in aqueous solutions with pH values of 5, 7, 11, and 14.

carried out, because of the aforementioned challenges in measuring thickness and contact resistance. Our data suggest that we successfully electrospun fiber mats from PEDOT:PSS-based precursors from acidic to neutral pH, without affecting their electrical properties.

We also evaluated the electrical properties of HighPEDOT2, HighPEDOT5, and HighPEDOT7 fiber mats, as shown in Figure S10. For the HighPEDOT2 fiber mats, the electric current varied from ∼0.01−1 μA, possibly due to variation in thickness and the adhesion of the fiber mats to the electrodes as discussed previously. However, when the pH value of the HighPEDOT precursor increased to 5.3 and 7.3 (HighPEDOT5 and HighPEDOT7), the electric current increased by 2 orders of magnitude (see Figures S10 and S11). We note that the reason for this increase was likely the appearance of precursor droplets on the electrodes. We suggest that the apparent precursor droplets flew off from the tip of the needle without developing Rayleigh instability or electrospraying. The distance between these droplets was too large to be observed using SEM. However, they significantly affected the electric measurement, as shown in Figure S11. This observation provides a pathway to remarkably increase the conductivity of the fiber mats by doping them with small droplets that potentially would not impact the porosity or mechanical properties of the fiber mats.

Electrical Properties of PEDOT:PSS-Based Fiber Mats as a Function of Relative Humidity

Understanding the performance of PEDOT:PSS-based fibers after exposure to different relative humidities is critical to knowing the different environments in which they could be used. For these experiments, we selected LowPEDOT3 fiber mats for preliminary studies due to the ease of sample preparation (i.e., no pH value modification to the solution precursor). As can be seen from Figure 6A, as the relative humidity increased up to 70%, the electrical current of the as-spun fiber mats decreased slightly, whereas it increased significantly at 90%. As the relative humidity increased (up to 70%), the absorption of water molecules by PSS swells the PSS chains and thus increases the distance between PEDOT chains making it more difficult for electrons to hop.[62,63] However, when the relative humidity increased above 90%, the ambient water condensed on the fiber mat and partially dissolved them due to their high content of water-soluble PVA, which led to a significant increase in the electrical current.

Thus, for situations where dissolution should be avoided, we cross-linked the LowPEDOT3 fibers with glutaraldehyde vapor and evaluated the effect of cross-linking. As can be seen from Figure S12, the cross-linking did not have any impact on fiber mat appearance including area coverage, fibrous morphology, and transparency (i.e., relative thickness). Moreover, as can be seen from the overlaid data plotted in Figure 6B for four different fiber mats, the electric current was equivalent for as-spun (closed symbols) and cross-linked (open symbols) fiber mats indicating that the cross-linking process did not impact the electrical conductivity either.

Stability of PEDOT:PSS-Based Fiber Mats' Electrical Properties Postwashing and Immersion Experiments

We also explored if there was any impact on electrical current after immersing the cross-linked LowPEDOT3 fiber mats in aqueous solutions with different pH values. We note that the as-spun fiber mats could not be used in these experiments, as they immediately dissolved upon immersion in solution. As can be seen from Figures 6C and S13, the electrical current decreased by ∼60−70% compared to cross-linked fiber mats after immersion in solutions that had pH values of 5, 7, and 11. However, after immersion in a pH 14 solution, the current decreased by 3 orders of magnitude. Increasing the pH value could have potentially changed the conformation and therefore, reduced the conductivity of the PEDOT polymer;[46] however, our Raman analysis for fibers postimmersion in solutions with pH values from 5 to 11 did not support this. We note that because immersing the fibers in pH = 14 solutions caused the cross-linked fibers to release from their substrates, they could not be analyzed using Raman. We hypothesize that the electric current might have decreased due to a decrease in the quantity of well-adhered fibers, diffusion of PEDOT:PSS from the cross-linked fibers into solution, and/or decrease in the conductivity of PEDOT postimmersion due to dedoping and/or change in conformation of PEDOT.

We performed Raman spectroscopy on as-spun and cross-linked fiber mats, as well as on fiber mats postimmersion in solutions with pH values from 5 to 11 (see Figure S14). For all of the fiber mats, we observed a peak at 1430 cm^{-1}, which indicates the presence of PEDOT within these fiber mats. We also observed that the width of the peak at 1430 cm^{-1} was the same for all fiber mats, regardless of the pH value of their precursor or the pH value of the immersion solution. This result is consistent with our electrical data as the pH value of precursor did not affect the electrical properties of fiber mats. Moreover, as the width of the peak remained the same postimmersion in pH 5 to 11 solutions, we suggest that the decrease in the current is most likely not due to the change in the conformation of PEDOT.

https://doi.org/10.1021/acsengineeringau.3c00044
ACS Eng. Au 2023, 3, 527−536

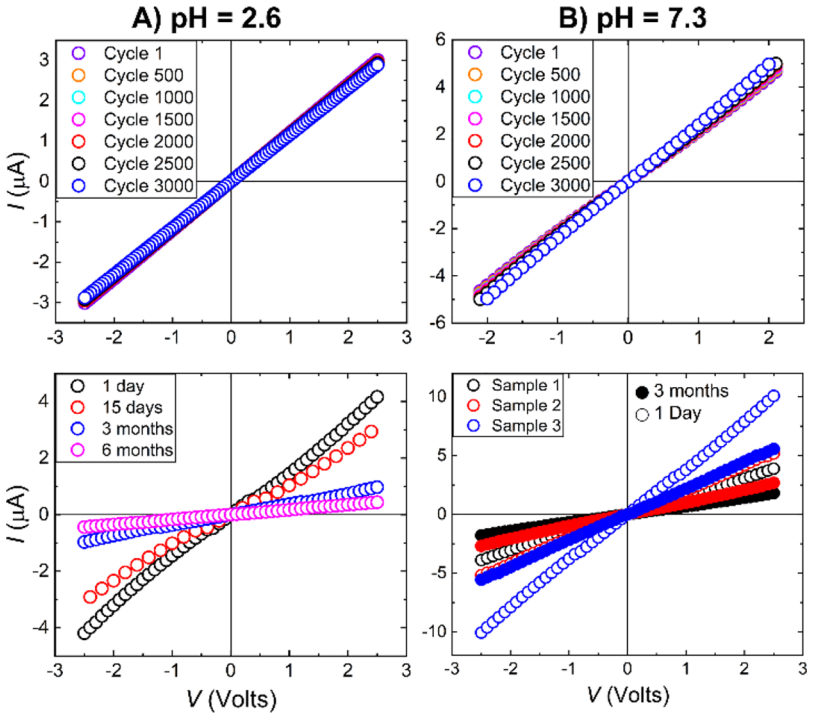

Figure 7. Electrical stability of as-spun (A) LowPEDOT3 and (B) LowPEDOT7 fiber mats (top) over 3000 cycles of voltage application as well as (bottom) multiple months of storage.

We also evaluated the electrical performance of the cross-linked LowPEDOT3 fiber mats before and after washing with soap water as shown in Figure S15 for two different samples. For *Sample 1*, the electrical current reduced by 40% after the first wash compared to the cross-linked fibers. However, upon the second wash, the reduction in the current was 18% compared to the first washing. Similarly, for *Sample 2*, the reduction in the electrical current was 55% and 20% for the first and second washes, respectively. Upon washing, it is possible that the PEDOT:PSS might diffuse out of the fibers because it is most likely physically trapped within the fibers and not chemically immobilized. This will affect the electrical stability of the fibers upon washing as well as upon immersion in different pH solutions. While ideally these fabrics could be washed many times without any loss, this preliminary evaluation suggests that the current decreased with subsequent washings and that the fabrics might be more appropriate for single wear applications (such as bandages). Notably, cross-linking (the PVA component of the fibers) enabled the ability to wash and reanalyze the same fiber mats. Future work could explore alternative cross-linking methods that completely avoid leakage of PEDOT from fibers because that would improve the mat's durability and electrical stability postwashing.

Electrical Properties after Long-Term Storage and Multiple Cycles of Current–Voltage Applications

We also examined the stability of the as-spun LowPEDOT3 and LowPEDOT7 fiber mats. Even after more than 3000 cycles of voltage applications, the current remained the same for both the LowPEDOT3 or LowPEDOT7 fiber mats (see Figure 7). These fiber mats were stored at room temperature and ambient relative humidity for 3 months before being reevaluated. Even though electrical current decreased for both LowPEDOT3 and LowPEDOT7 fiber mats, the reduction was ∼50% for LowPEDOT7 fiber mats compared to >75% for LowPEDOT3 (see Figure 7, bottom). This long-term storage study indicates that more stable fiber mats were obtained from precursor electrospun from the less acidic precursors.

CONCLUSION

In this study, we have electrospun PEDOT:PSS/PVA nanofibers by adjusting the pH of the precursors by adding NaOH. We found that electrospinnability and electrical properties, were not impacted when the pH became slightly basic (pH = 7.3). We also explored the performance of the fibers after cross-linking, exposure to different pH value solutions, as well as washing with agitated soap water. The electrical current was retained after glutaraldehyde vapor cross-linking, but it decreased by a factor of 3 upon immersion in solutions with pH values of 5 to 11. Moreover, the reduction in current after the first wash with soap water compared to cross-linked fiber mat was ∼50%. Our results indicate that PEDOT:PSS/PVA fibers are suitable for applications requiring exposure to acidic or basic environments. We also evaluated their stability for long-term storage and found that fiber mats obtained from less acidic precursors are more stable. Future work to improve these fabrics toward wearable devices could explore alternative cross-linking methods, which would provide more electrical stability postimmersion and multiple washings of the fabrics.

ASSOCIATED CONTENT

Supporting Information

The Supporting Information is available free of charge at https://pubs.acs.org/doi/10.1021/acsengineeringau.3c00044.

Experimental setup, digital images of gelled precursors, electrospun fiber morphology (brightfield microscopy, SEM micrographs, analysis), electrical (current–voltage) data for electrospun fibers, washing stability data, Raman spectroscopy data (PDF)

https://doi.org/10.1021/acsengineeringau.3c00044
ACS Eng. Au 2023, 3, 527–536

AUTHOR INFORMATION

Corresponding Author

Jessica D. Schiffman − *Department of Chemical Engineering, University of Massachusetts Amherst, Amherst, Massachusetts 01003-9303, United States;* orcid.org/0000-0002-1265-5392; Email: schiffman@umass.edu

Author

Prerana Rathore − *Department of Chemical Engineering, University of Massachusetts Amherst, Amherst, Massachusetts 01003-9303, United States;* orcid.org/0000-0002-9797-9766

Complete contact information is available at: https://pubs.acs.org/10.1021/acsengineeringau.3c00044

Author Contributions

CRediT: **Prerana Rathore** conceptualization, data curation, formal analysis, writing-original draft, writing-review & editing; **Jessica D. Schiffman** conceptualization, formal analysis, funding acquisition, project administration, resources, supervision, writing-original draft, writing-review & editing.

Notes

The authors declare no competing financial interest.

ACKNOWLEDGMENTS

The authors thank Jana Latayan and Elana Peisner for preliminary discussions. Thanks to Dr. Reika Katsumata and Dr. Sarah L. Perry for allowing us to use their Raman spectrometer and brightfield microscope, respectively. The authors acknowledge the support from the National Science Foundation (Award #1921839). P.R. acknowledges support from the Douglas Fellowship. We acknowledge the facilities at the W.M. Keck Center for Electron Microscopy and the roll-2-roll fabrication facility within the UMass Institute of Applied Life Science.

REFERENCES

(1) Wang, J. P.; Xue, P.; Tao, X. M. Strain Sensing Behavior of Electrically Conductive Fibers under Large Deformation. *Mater. Sci. Eng., A* **2011**, *528* (6), 2863−2869.

(2) Leote, R. J. B.; Beregoi, M.; Enculescu, I.; Diculescu, V. C. Metallized Electrospun Polymeric Fibers for Electrochemical Sensors and Actuators. *Curr. Opin. Electrochem.* **2022**, *34*, No. 101024.

(3) Lu, Y.; Biswas, M. C.; Guo, Z.; Jeon, J.-W.; Wujcik, E. K. Recent Developments in Bio-Monitoring via Advanced Polymer Nanocomposite-Based Wearable Strain Sensors. *Biosens. Bioelectron.* **2019**, *123*, 167−177.

(4) Filho, G.; Júnior, C.; Spinelli, B.; Damasceno, I.; Fiuza, F.; Morya, E. All-Polymeric Electrode Based on PEDOT:PSS for In Vivo Neural Recording. *Biosensors* **2022**, *12* (10), 853.

(5) Tee, B. C.-K.; Wang, C.; Allen, R.; Bao, Z. An Electrically and Mechanically Self-Healing Composite with Pressure- and Flexion-Sensitive Properties for Electronic Skin Applications. *Nat. Nanotechnol.* **2012**, *7* (12), 825−832.

(6) Ohm, Y.; Pan, C.; Ford, M. J.; Huang, X.; Liao, J.; Majidi, C. An Electrically Conductive Silver−Polyacrylamide−Alginate Hydrogel Composite for Soft Electronics. *Nat. Electron.* **2021**, *4* (3), 185−192.

(7) Ma, X.; Li, W.; Wang, L.; Cao, X. Electric Conductivity and Piezoresistivity of Carbon Nanotube Artificial Skin Based on the Design of Mesh Structure. *Adv. Mater. Sci. Eng.* **2018**, *2018*, No. 9846389.

(8) Wicaksono, I.; Tucker, C. I.; Sun, T.; Guerrero, C. A.; Liu, C.; Woo, W. M.; Pence, E. J.; Dagdeviren, C. A Tailored, Electronic Textile Conformable Suit for Large-Scale Spatiotemporal Physiological Sensing in Vivo. *npj Flex. Electron.* **2020**, *4* (1), 5.

(9) Huang, Z. M.; Zhang, Y.-Z.; Kotaki, M.; Ramakrishna, S. A Review on Polymer Nanofibers by Electrospinning and Their Applications in Nanocomposites. *Compos. Sci. Technol.* **2003**, *63* (15), 2223−2253.

(10) Deitzel, J. M.; Kleinmeyer, J.; Harris, D.; Beck Tan, N. C. The Effect of Processing Variables on the Morphology of Electrospun Nanofibers and Textiles. *Polymer* **2001**, *42* (1), 261−272.

(11) Teo, W. E.; Ramakrishna, S. A Review on Electrospinning Design and Nanofibre Assemblies. *Nanotechnology* **2006**, *17* (14), R89.

(12) Ramakrishna, S.; Fujihara, K.; Teo, W. E.; Lim, T. C.; Ma, Z. Functionalization of Plymer Nanofibers. In *An Introduction to Electrospinning and Nanofibers*; World Scientific, 2005; pp 247−274.

(13) Ge, J. J.; Hou, H.; Li, Q.; Graham, M. J.; Greiner, A.; Reneker, D. H.; Harris, F. W.; Cheng, S. Z. D. Assembly of Well-Aligned Multiwalled Carbon Nanotubes in Confined Polyacrylonitrile Environments: Electrospun Composite Nanofiber Sheets. *J. Am. Chem. Soc.* **2004**, *126* (48), 15754−15761.

(14) Dror, Y.; Salalha, W.; Khalfin, R. L.; Cohen, Y.; Yarin, A. L.; Zussman, E. Carbon Nanotubes Embedded in Oriented Polymer Nanofibers by Electrospinning. *Langmuir* **2003**, *19* (17), 7012−7020.

(15) Song, J.; Chen, M.; Olesen, M. B.; Wang, C.; Havelund, R.; Li, Q.; Xie, E.; Yang, R.; Bøggild, P.; Wang, C.; Besenbacher, F.; Dong, M. Direct Electrospinning of Ag/Polyvinylpyrrolidone Nanocables. *Nanoscale* **2011**, *3* (12), 4966−4971.

(16) Yanılmaz, M.; Sarac, A. S. A Review: Effect of Conductive Polymers on the Conductivities of Electrospun Mats. *Text. Res. J.* **2014**, *84* (12), 1325−1342.

(17) Luzio, A.; Canesi, E. V.; Bertarelli, C.; Caironi, M. Electrospun Polymer Fibers for Electronic Applications. *Materials* **2014**, *7* (2), 906−947.

(18) Gueye, M. N.; Carella, A.; Faure-Vincent, J.; Demadrille, R.; Simonato, J.-P. Progress in Understanding Structure and Transport Properties of PEDOT-Based Materials: A Critical Review. *Prog. Mater. Sci.* **2020**, *108*, No. 100616.

(19) Sun, K.; Zhang, S.; Li, P.; Xia, Y.; Zhang, X.; Du, D.; Isikgor, F. H.; Ouyang, J. Review on Application of PEDOTs and PEDOT:PSS in Energy Conversion and Storage Devices. *J. Mater. Sci. Mater. Electron.* **2015**, *26* (7), 4438−4462.

(20) Cao, G.; Cai, S.; Chen, Y.; Zhou, D.; Zhang, H.; Tian, Y. Facile Synthesis of Highly Conductive and Dispersible PEDOT Particles. *Polymer* **2022**, *252*, No. 124952.

(21) Nie, S.; Li, Z.; Yao, Y.; Jin, Y. Progress in Synthesis of Conductive Polymer Poly(3,4-Ethylenedioxythiophene. *Front. Chem.* **2021**, *9*, No. 803509.

(22) Lang, U.; Müller, E.; Naujoks, N.; Dual, J. Microscopical Investigations of PEDOT:PSS Thin Films. *Adv. Funct. Mater.* **2009**, *19* (8), 1215−1220.

(23) Huang, Y.-C.; Lo, T.-Y.; Chen, C.-H.; Wu, K.-H.; Lin, C.-M.; Whang, W.-T. Electrospinning of Magnesium-Ion Linked Binder-Less PEDOT:PSS Nanofibers for Sensing Organic Gases. *Sens. Actuators B Chem.* **2015**, *216*, 603−607.

(24) Zhang, H.-D.; Yan, X.; Zhang, Z.-H.; Yu, G.-F.; Han, W.-P.; Zhang, J.-C.; Long, Y.-Z. Electrospun PEDOT:PSS/PVP Nanofibers for CO Gas Sensing with Quartz Crystal Microbalance Technique. *Int. J. Polym. Sci.* **2016**, *2016*, No. 3021353.

(25) Zhang, Q.; Wang, X.; Fu, J.; Liu, R.; He, H.; Ma, J.; Yu, M.; Ramakrishna, S.; Long, Y. Electrospinning of Ultrafine Conducting Polymer Composite Nanofibers with Diameter Less than 70 Nm as High Sensitive Gas Sensor. *Materials* **2018**, *11* (9), 1744.

(26) Regmi, A.; Shin, D.; Na, N.; Chang, J. Suspended Graphene/PEDOT: PSS-PEO Channel for H_2 Gas Sensing Fabricated Using Direct-Write Functional Fibers. *Adv. Mater. Technol.* **2023**, *8* (7), No. 2201505.

(27) Shaker, A.; Hassanin, A. H.; Shaalan, N. M.; Hassan, M. A.; El-Moneim, A. A. Micropatterned Flexible Strain Gauge Sensor Based on

Wet Electrospun Polyurethane/PEDOT: PSS Nanofibers. *Smart Mater. Struct.* **2019**, *28* (7), No. 075029.
(28) Fallahi, A.; Mandla, S.; Kerr-Phillip, T.; Seo, J.; Rodrigues, R. O.; Jodat, Y. A.; Samanipour, R.; Hussain, M. A.; Lee, C. K.; Bae, H.; Khademhosseini, A.; Travas-Sejdic, J.; Shin, S. R. Flexible and Stretchable PEDOT-Embedded Hybrid Substrates for Bioengineering and Sensory Applications. *ChemNanoMat* **2019**, *5* (6), 729−737.
(29) Julian, T.; Rianjanu, A.; Hidayat, S. N.; Kusumaatmaja, A.; Roto, R.; Triyana, K. Quartz Crystal Microbalance Coated with PEDOT−PSS/PVA Nanofiber for a High-Performance Humidity Sensor. *J. Sens. Sens. Syst.* **2019**, *8* (2), 243−250.
(30) Kim, S.; Lee, K. Y.; Lim, J.-H. Fabrication of PEDOT: PSS-PVP Nanofiber-Embedded Sb_2Te_3 Thermoelectric Films by Multi-Step Coating and Their Improved Thermoelectric Properties. *Materials* **2020**, *13* (12), 2835.
(31) Jin, S.; Sun, T.; Fan, Y.; Wang, L.; Zhu, M.; Yang, J.; Jiang, W. Synthesis of Freestanding PEDOT:PSS/PVA@Ag NPs Nanofiber Film for High-Performance Flexible Thermoelectric Generator. *Polymer* **2019**, *167*, 102−108.
(32) Jiang, X.; Ban, C.; Li, L.; Hao, J.; Shi, N.; Chen, W.; Gao, P. Electrospinning of BCNNTs/PVA/PEDOT Composite Nanofibers Films for Research Thermoelectric Performance. *J. Appl. Polym. Sci.* **2022**, *139* (17), 52049.
(33) Park, S. W.; Oh, T. H.; Hwang, J. S.; Lee, Y. J. Effect of Solvent and Blended Polymer on Electrical Conductivity of PEDOT:PSS/Polymer Blended Nanofibers. *Fibers Polym.* **2016**, *17* (8), 1171−1174.
(34) Yin, J.; Bai, Y.; Lu, J.; Ma, J.; Zhang, Q.; Hong, W.; Jiao, T. Enhanced Mechanical Performances and High-Conductivity of rGO/PEDOT:PSS/PVA Composite Fiber Films via Electrospinning Strategy. *Colloids Surf. A Physicochem. Eng.* **2022**, *643*, No. 128791.
(35) Chotimah; Winandianto, B.; Munir, M.; Kartini, I.; Kusumaatmaja, A.; Triyana, K. The Electrical Properties of PEDOT:PSS Nanofibers. *AIP Conf. Proc.* **2016**, *1755* (1), No. 150013.
(36) Zhao, W.; Yalcin, B.; Cakmak, M. Dynamic Assembly of Electrically Conductive PEDOT:PSS Nanofibers in Electrospinning Process Studied by High Speed Video. *Synth. Met.* **2015**, *203*, 107−116.
(37) Moreno-Cortez, I. E.; Alvarado-Castañeda, A.; Garcia-Gutierrez, D. F.; Garcia-Gomez, N. A.; Sepulveda-Guzman, S.; Garcia-Gutierrez, D. I. Core−Shell PEDOT:PSS—PVP Nanofibers Containing PbS Nanoparticles through Coaxial Electrospinning. *Synth. Met.* **2016**, *220*, 255−262.
(38) Mendoza-Diaz, M. I.; Garcia-Gutierrez, D. F.; Sepulveda-Guzman, S.; Moreno-Cortez, I. E.; Garcia-Gutierrez, D. I. Tuning the Optoelectronic Properties of PEDOT:PSS-PVP Core−Shell Electrospun Nanofibers by Solvent-Quantum Dot Doping and Phase Inversion. *Nanotechnology* **2019**, *30* (39), No. 395601.
(39) Bessaire, B.; Mathieu, M.; Salles, V.; Yeghoyan, T.; Celle, C.; Simonato, J. P.; Brioude, A. Synthesis of Continuous Conductive PEDOT: PSS Nanofibers by Electrospinning: A Conformal Coating for Optoelectronics. *ACS Appl. Mater. Interfaces* **2017**, *9* (1), 950−957.
(40) Cárdenas-Martínez, J.; España-Sánchez, B. L.; Esparza, R.; Ávila-Niño, J. A. Flexible and Transparent Supercapacitors Using Electrospun PEDOT:PSS Electrodes. *Synth. Met.* **2020**, *267*, No. 116436.
(41) Cameron, J.; Skabara, P. J. The Damaging Effects of the Acidity in PEDOT:PSS on Semiconductor Device Performance and Solutions Based on Non-Acidic Alternatives. *Mater. Horiz.* **2020**, *7* (7), 1759−1772.
(42) de Jong, M. P.; van IJzendoorn, L. J.; de Voigt, M. J. A. Stability of the Interface between Indium-Tin-Oxide and Poly(3,4-Ethylenedioxythiophene)/Poly(Styrenesulfonate) in Polymer Light-Emitting Diodes. *Appl. Phys. Lett.* **2000**, *77* (14), 2255−2257.
(43) van Dijken, A.; Perro, A.; Meulenkamp, E. A.; Brunner, K. The Influence of a PEDOT:PSS Layer on the Efficiency of a Polymer Light-Emitting Diode. *Org. Electron.* **2003**, *4* (2−3), 131−141.
(44) Baranoff, E.; Curchod, B. F. E.; Frey, J.; Scopelliti, R.; Kessler, F.; Tavernelli, I.; Rothlisberger, U.; Grätzel, M.; Nazeeruddin, Md. K. Acid-Induced Degradation of Phosphorescent Dopants for OLEDs and Its Application to the Synthesis of Tris-Heteroleptic Iridium(III) Bis-Cyclometalated Complexes. *Inorg. Chem.* **2012**, *51* (1), 215−224.
(45) Bhargav, R.; Bhardwaj, D.; Shahjad; Patra, A.; Chand, S. Poly(Styrene Sulfonate) Free Poly(3,4-Ethylenedioxythiophene) as a Robust and Solution-Processable Hole Transport Layer for Organic Solar Cells. *ChemistrySelect* **2016**, *1* (7), 1347−1352.
(46) Mochizuki, Y.; Horii, T.; Okuzaki, H. Effect of pH on Structure and Conductivity of PEDOT/PSS. *Trans. Mater. Res. Soc. Jpn.* **2012**, *37* (2), 307−310.
(47) Hofmann, A. I.; Smaal, W. T. T.; Mumtaz, M.; Katsigiannopoulos, D.; Brochon, C.; Schütze, F.; Hild, O. R.; Cloutet, E.; Hadziioannou, G. An Alternative Anionic Polyelectrolyte for Aqueous PEDOT Dispersions: Toward Printable Transparent Electrodes. *Angew. Chem.* **2015**, *127* (29), 8626−8630.
(48) Zarrin, N.; Tavanai, H.; Abdolmaleki, A.; Bazarganipour, M.; Alihosseini, F. An Investigation on the Fabrication of Conductive Polyethylene Dioxythiophene (PEDOT) Nanofibers through Electrospinning. *Synth. Met.* **2018**, *244*, 143−149.
(49) Laforgue, A.; Robitaille, L. Production of Conductive PEDOT Nanofibers by the Combination of Electrospinning and Vapor-Phase Polymerization. *Macromolecules* **2010**, *43* (9), 4194−4200.
(50) Jin, L.; Wang, T.; Feng, Z.-Q.; Leach, M. K.; Wu, J.; Mo, S.; Jiang, Q. A Facile Approach for the Fabrication of Core−Shell PEDOT Nanofiber Mats with Superior Mechanical Properties and Biocompatibility. *J. Mater. Chem. B* **2013**, *1* (13), 1818.
(51) Destaye, A. G.; Lin, C.-K.; Lee, C.-K. Glutaraldehyde Vapor Cross-Linked Nanofibrous PVA Mat with in Situ Formed Silver Nanoparticles. *ACS Appl. Mater. Interfaces* **2013**, *5* (11), 4745−4752.
(52) Schiffman, J. D.; Schauer, C. L. Cross-Linking Chitosan Nanofibers. *Biomacromolecules* **2007**, *8* (2), 594−601.
(53) Greenspan, L. Humidity Fixed Points of Binary Saturated Aqueous Solutions. *J. Res. Natl. Bur. Stand. Sect. A* **1977**, *81A* (1), 89.
(54) Kasselkus, A.; Weiskircher-Hildebrandt, E.; Schornick, E.; Bauer, F.; Zheng, M. Polyvinyl Alcohol: Revival of a Long Lost Polymer. EMDMillipore White Paper, 2018, pp 116. https://www.bioprocessonline.com/doc/polyvinyl-alcohol-revival-of-a-long-lost-polymer-0001.
(55) Ramakrishna, S.; Fujihara, K.; Teo, W. E.; Lim, T. C.; Ma, Z. Electrospinning Process. In *An Introduction to Electrospinning and Nanofibers*; World Scientific, 2005; pp 90−154.
(56) Zander, N. E. Hierarchically Structured Electrospun Fibers. *Polymers* **2013**, *5* (1), 19−44.
(57) Rathore, P.; Schiffman, J. D. Beyond the Single-Nozzle: Coaxial Electrospinning Enables Innovative Nanofiber Chemistries, Geometries, and Applications. *ACS Appl. Mater. Interfaces* **2021**, *13* (1), 48−66.
(58) Shi, Q.; Fan, Q.; Xu, X.; Ye, W.; Hou, J.; Wong, S.-C.; Yin, J. Effect of Surface Interactions on Adhesion of Electrospun Meshes on Substrates. *Langmuir* **2014**, *30* (45), 13549−13555.
(59) Amini, G.; Gharehaghaji, A. A. Improving Adhesion of Electrospun Nanofiber Mats to Supporting Substrate by Using Adhesive Bonding. *Int. J. Adhes. Adhes.* **2018**, *86*, 40−44.
(60) Zhang, B.; Yan, X.; Xu, Y.; Zhao, H.-S.; Yu, M.; Long, Y.-Z. Measurement of Adhesion of *In Situ* Electrospun Nanofibers on Different Substrates by a Direct Pulling Method. *Adv. Mater. Sci. Eng.* **2020**, *2020*, No. 7517109.
(61) Amini, G.; Samiee, S.; Gharehaghaji, A. A.; Hajiani, F. Fabrication of Polyurethane and Nylon 66 Hybrid Electrospun Nanofiber Layer for Waterproof Clothing Applications. *Adv. Polym. Technol.* **2016**, *35* (4), No. 419.
(62) Kuş, M.; Okur, S. Electrical Characterization of PEDOT:PSS beyond Humidity Saturation. *Sens. Actuators B Chem.* **2009**, *143* (1), 177−181.
(63) Benchirouf, A.; Palaniyappan, S.; Ramalingame, R.; Raghunandan, P.; Jagemann, T.; Müller, C.; Hietschold, M.; Kanoun, O. Electrical Properties of Multi-Walled Carbon Nano-

tubes/PEDOT:PSS Nanocomposites Thin Films Under Temperature and Humidity Effects. *Sens. Actuators B Chem.* **2016**, *224*, 344−350.

https://doi.org/10.1021/acsengineeringau.3c00044
ACS Eng. Au 2023, 3, 527−536